Fiber-based multiple access timing signal synchronization technique*

Yi-Bo Yuan(袁一博)[1,3], Bo Wang(王波)[1,2,†], Chao Gao(高超)[1,2], and Li-Jun Wang(王力军)[1,2,3]

[1] *Joint Institute for Measurement Science, State Key Laboratory of Precision Measurement Technology and Instruments, Tsinghua University, Beijing* 100084, *China*

[2] *Department of Precision Instrument, Tsinghua University, Beijing* 100084, *China*

[3] *Department of Physics, Tsinghua University, Beijing* 100084, *China*

(Received 23 September 2016; revised manuscript received 29 November 2016; published online 10 March 2017)

A fiber-based, multiple access timing signal synchronization scheme is demonstrated. By coupling out the bidirectional transmission signals, a highly stable timing signal can be recovered at arbitrary points along the fiber with the help of the loop delay message broadcasted via ethernet from the local module. The experiment is carried out on a 30-km fiber placed in a temperature-controlled box. In one-day period, when the round trip fiber transfer delay fluctuation is 60 ns, the fluctuations of the stabilized timing signal from the download and the remote modules were only ±125 ps and ±100 ps, respectively. Also, the system error caused by transmission path asymmetry and thermal drift is calibrated, and a 100-ps magnitude synchronization accuracy is realized. This method could provide new insights into the construction of a fiber-based time transfer network.

Keywords: time synchronization, multiple access, time transfer

PACS: 06.30.–k, 07.60.Vg, 06.30.Ft **DOI:** 10.1088/1674-1056/26/4/040601

1. Introduction

Time and frequency dissemination via fiber link has properties of low losses, isolation to electro-magnetic interference, easily availability and is highly reliable. It is considered to be a promising technique to construct a large scale time and frequency network.[1–3] Different topological structures of fiber-based time and frequency dissemination schemes such as point-to-point, multiple access, cascade and star shape, have been demonstrated. For frequency dissemination, the point-to-point scheme[4–10] is mainly used by scientific laboratories to compare atomic frequency standards. To realize long-distance frequency dissemination, the cascaded frequency dissemination method has been studied.[11–13] Aiming towards applications in frequency synchronization networks, multiple access,[14–19] and star-topology[20–22] frequency dissemination methods have been proposed and demonstrated. For dissemination of timing signals, a point-to-point scheme is usually realized in a way as a variant of Two Way Satellite Time and Frequency Transfer (TWSTFT)[23–26] or by compensating the loop delay fluctuation.[27–32] To extend its applications in the complicated network topology, different multiple access timing signal synchronization schemes have been demonstrated.[33,34] For these schemes, to recover a stable timing signal at client points, the loop delay have to be measured and compensated at the transmitting site firstly. Once a failure happens to the transmitting site compensation function, the whole synchronization system will be broken down. To improve the system reliability, in the proposed scheme, we share the complexities and risks among transmitting and client modules by setting the compensation function at client modules. In this way, if one client module compensation function is broken, other client modules can still be running normally. Recently, client side compensated frequency dissemination schemes with good reliability and performance also have been demonstrated.[18,19,35,36]

In this paper, we demonstrate a fiber-based multi-access timing signal synchronization scheme which does not need transfer delay compensation at the transmitting module. Recently, Chen *et al.*[21] realized tree-like client side compensation time transfer network in a different way. At remote sites, they acquired single trip time delay by distinguishing uplink and downlink timing signal with Wavelength Division Multiplex (WDM) technology. While in our scheme at the transmitting module the round trip transfer delay is measured and broadcast via ethernet, and the compensation function is set at the client modules (remote and download ones). With the help of the received message from the ethernet, stable timing signals can be recovered at client modules. In this way, a timing signal dissemination stability of ±125 ps and ±100 ps was achieved at the download and remote modules, respectively. Also, we calibrated the synchronization system, and eliminated the systematic error caused by the loop asymmetry and thermal drift. Finally, synchronization of the timing signal was realized.

2. Method and experimental results

Figure 1(a) shows a schematic illustration of the multiple access timing signal synchronization system, which consists

*Project supported by the National Key Scientific Instrument and Equipment Development Project of China (Grant No. 2013YQ09094303) and the Program of International Science and Technology Cooperation (Grant No. 2016YFE0100200).

†Corresponding author. E-mail: bo.wang@tsinghua.edu.cn

© 2017 Chinese Physical Society and IOP Publishing Ltd

of one local and two client modules. These three modules are linked by two fiber spools that are 25-km and 5-km long. Using a 2×2 fiber coupler (coupler1, coupling ratio 50:50), forward and backward transmitted laser light in the fiber link can be outcoupled at the download module. Figures 1(b)–1(d) show the details of local, download, and remote modules, respectively. At the local module, the timing signal is generated by a synthesized clock generator referenced to a hydrogen-maser. The repetition rate of the timing signal is 500 Hz with a 1:1 duty ratio. It is used to modulate the amplitude of 1550-nm laser carrier, then it is disseminated to the download and remote modules. The received timing signal is amplified and sent backward at the remote module, while the download module can retrieve the bidirectional transmission signals. Due to the Rayleigh backscattering noises, the demodulated timing signal will be jittery. To decrease its influence, the gain of the EDFAs and the trigger level of electrical instruments (TICs and controlled delay boxes) should be carefully adjusted. At the local module, computer 1 acquires the round trip delay measured by Time Interval Counter 1 (TIC1, all the Time Interval Counter used in the scheme is Keysight 53230A) and broadcasts it to the download and remote modules via ethernet. At the client modules, two controlled delay boxes (DG535 from Stanford Research Systems) can compensate for the fiber transfer delay fluctuations accordingly.

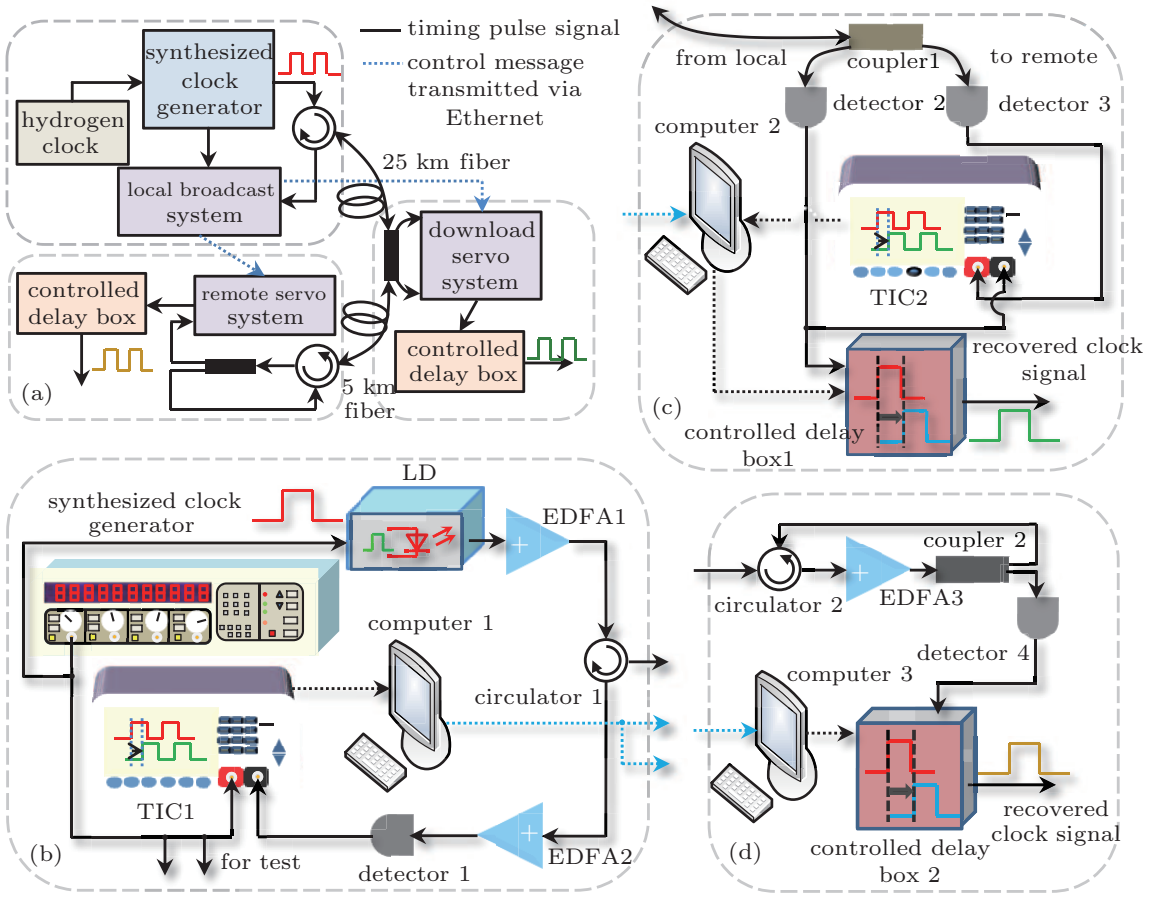


Fig. 1. (color online) (a) A schematic illustration of the multiple access timing signal dissemination system. (b) The local module. (c) The download module. (d) The remote module. LD: laser diode. TIC: time interval counter. EDFA: erbium-doped fiber amplifier.

Assuming that the uplink and downlink transmission time delay are equivalent and ignoring the induced time delay of the three modules' apparatuses, the result measured by the TIC1 can be expressed as

$$T_1 = 2 \times (T_{25\ \mathrm{km}} + T_{5\ \mathrm{km}}), \tag{1}$$

where $T_{25\ \mathrm{km}}$ is the transfer delay of the 25-km fiber spool and $T_{5\ \mathrm{km}}$ is the transfer delay of the 5-km fiber spool. The time difference between the retrieved bidirectional transmission signals measured by TIC2 is

$$T_2 = 2 \times T_{5\ \mathrm{km}}. \tag{2}$$

Consequently, the time difference between the retrieved backward signal at the download module and the clock signal at the local module is $T_{25\ \mathrm{km}} + 2T_{5\ \mathrm{km}}$, which equals to $0.5(T_1 + T_2)$. In this way, the time difference between the local and download modules can be determined. Triggered by the retrieved backward signal, controlled delay box1 can recover a square pulse with a 5-ps time delay resolution. Instead of stabilizing the fiber link, the controlled delay box is utilized as the compensation part of servo system to stabilize the timing signal. Considering the set delay at controlled delay box 1 is $\Delta T_{\mathrm{box\ 1}}$, the time difference between the recovered clock sig-

nal at the download module and the clock signal at the local module is T_{LtoD} and it equals to $0.5(T_1+T_2)+\Delta T_{\mathrm{box\ 1}}$. To keep T_{LtoD} constant, $\Delta T_{\mathrm{box\ 1}}$ should be controlled according to the change in $0.5(T_1+T_2)$. This stabilizes the recovered clock signal at the download module. Similarly, the time delay between the received timing signal at the remote module and the clock signal at the local module is $T_{25\ \mathrm{km}}+T_{5\ \mathrm{km}}$, which equals $0.5T_1$. By adjusting control controlled delay box 2 and keeping $T_{\mathrm{LtoR}}=0.5T_1+\Delta T_{\mathrm{box\ 2}}$ constant, a stable clock signal can also be recovered at the remote module. Here T_{LtoR} is the time difference between the recovered clock signal at the download module and the clock signal at the local module and $\Delta T_{\mathrm{box\ 2}}$ is the set delay at controlled delay box 2. During the experiment, the acquisition rates of TIC1 and TIC2 were set to 500 Hz, for an average time of 1 s. Taking factors such as the data acquisition time, the ethernet transmission time and the instrument response time into consideration, to ensure enough margin, the feedback loop time was set to 2 s. Furthermore, the round trip delay message is set to highest priority by configuring the router of the Ethernet, and broadcasts from transmitting module to all clients. Consequently, the influence of the Ethernet congestion can be greatly minimized in our experimental demonstration.

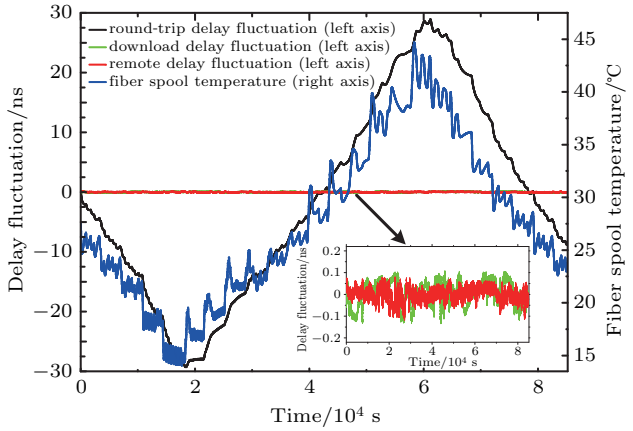


Fig. 2. (color online) Double Y plot of temperature and measured time delay fluctuations over one day. Black line: the transfer delay fluctuations of the round trip fiber. Green line: time delay fluctuations of the recovered timing signal at download module. Red line: time delay fluctuations of the recovered timing signal at remote module. Blue line: the temperature fluctuations of the fiber spools.

To test the stability of the timing signal dissemination, two fiber spools were placed in a temperature-controlled box. The black curve in Fig. 3 shows the transfer delay fluctuation of the round trip fiber measured by TIC1 when the temperature was varied between 15 °C and 40 °C. Over one day, the round-trip delay fluctuation of the 30-km fiber link was 60 ns. To evaluate the performance of the system, the recovered timing signal at the remote and download modules were compared with a local module clock signal with a 1-s averaging time, and are represented by the red and green lines in Fig. 2. The test results are normalized, which means that only the variation is expressed and the mean values are set to zero. The delay fluctuation of the remote module was less than ±100 ps and that of the download m was less than ±125 ps.

3. Error analysis and the calibration of experimental apparatus

Using the above mentioned method, we can obtain a highly stabilized timing signal at client modules. To realize time synchronization, the system error should be determined and eliminated. For example, the controlled delay box has an intrinsic dead time delay T_{dr}, which is 80 ns to 90 ns. Therefore, the time delay between the input trigger and the recovered signal is T_{box} which equals to $T_{\mathrm{dr}}+T_{\mathrm{set}}$, where T_{set} is the delay value, which can be adjusted with 5-ps resolution. However, the delay of the optical components may also contribute to the system transmission asymmetry, which also results in synchronization inaccuracy. The wrong estimate of the absolute value of T_{LtoD} and T_{LtoR} caused by the system transmission asymmetry can be expressed as $T_{\mathrm{asydownload}}$ at download module and $T_{\mathrm{asyremote}}$ at remote module, respectively. $T_{\mathrm{asydownload}}$ and $T_{\mathrm{asyremote}}$ are mainly induced by the asymmetric assignment of utilized components. Consequently, for the download module, the modified time delay of the recovered timing signal behind the local module is $0.5(T_1+T_2)+T_{\mathrm{asydownload}}+T_{\mathrm{dr1}}$. For the remote module, the modified delay is $0.5T_1+T_{\mathrm{asyremote}}+T_{\mathrm{dr2}}$. Once the accurate values of $T_{\mathrm{asydownload}}$, $T_{\mathrm{asyremote}}$, T_{dr1}, and T_{dr2} are determined, then accurate time synchronization can be realized.

We used two methods, the integrated calibration method and separated calibration method, to calibrate the system transmission asymmetry and compare the results. For the integrated calibration method, at first, we spliced the local, download and remote modules. Figure 3(a) shows the integrated method used to calibrate $T_{\mathrm{asydownload}}$. TIC3 is used to measure T_3, which is the true value of the time delay of the retrieved timing signal at the download module behind the local module. $T_{\mathrm{asydownload}}$ is equal to $T_3-0.5(T_1+T_2)$, which is the transmission asymmetry of the download module. Secondly, figure 3(b) shows the integrated method used to calibrate $T_{\mathrm{asyremote}}$. TIC4 is used to measure the true value of the remote module time delay T_4. $T_{\mathrm{asyremote}}$ is given by $T_4-0.5T_1$, which is the transmission asymmetry of the remote module. At the same time, the thermal drift of the devices was evaluated and calibrated. During the calibration, experimental devices shown in Figs. 3(a) and 3(b) were placed in a temperature-controlled box where the temperature was varied from 20 °C to 30 °C. The measured $T_{\mathrm{asydownload}}$ and $T_{\mathrm{asyremote}}$ along with the variation in temperature were recorded. By linearly fitting the acquired data, the thermal drift relationship of $T_{\mathrm{asydownload}}(t)$ and $T_{\mathrm{asyremote}}(t)$ can be obtained as shown in Figs. 4(a) and 4(b). In the diagrams, all measured samples are represented by the shaded area and the mean values are represented by solid lines within the shaded areas.

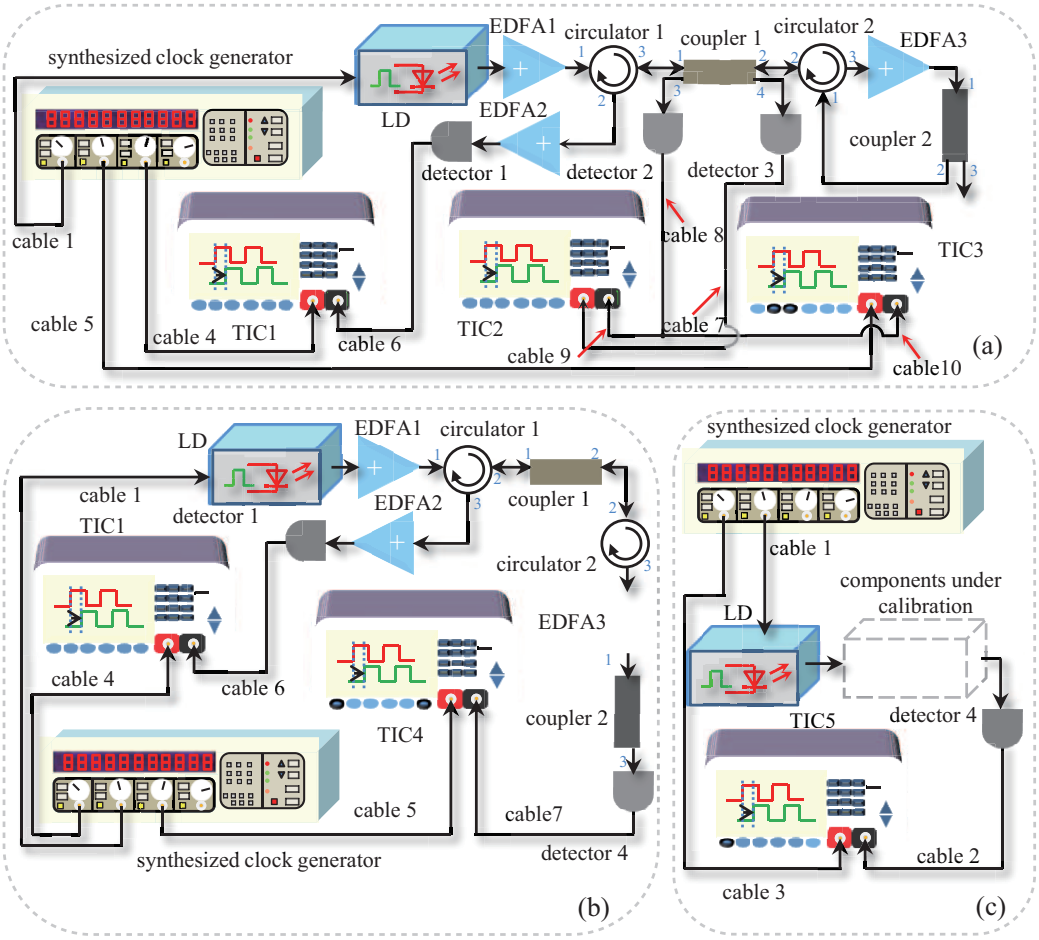


Fig. 3. (color online) A schematic illustration of the two transmission asymmetry calibration methods: (a) the download module integrated calibration method; (b) the remote module integrated calibration method; (c) the separated calibration method using an LD-detector pair. All fiber pigtails are included in the components and all the signal cables used are also marked.

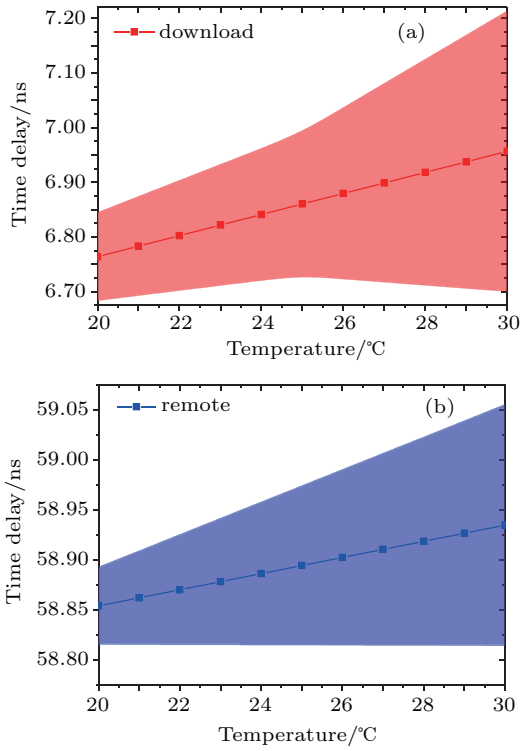


Fig. 4. (color online) Results of the integrated calibration method: (a) download module calibration results; (b) remote module calibration results.

In practical applications, the temperature of the three modules may be different, or the calibration process may not be undertaken at the same place because the fiber link has already been deployed. Consequently, the separated calibration method is used to obtain the asymmetry values by calibrating all components one by one. To obtain $T_{\text{asydownload}}$ and $T_{\text{asyremote}}$, the results of the calibration of individual components are accumulated according to the system arrangement. The results of the two methods can be compared with each other to demonstrate their calibration accuracy. The separated calibration scheme of the individual components is shown in Fig. 3(c). Each of the optical components, including the optical couplers, Erbium Doped Fiber Amplifiers (EDFAs), optical circulators and Laser Diode (LD)-detector pairs were calibrated under different environmental temperatures with the help of TIC5 according to the scheme. At first, the calibration of the LD-detector pairs was performed. Secondly other components were calibrated by subtracting the contribution of the LD-detector pair. Thirdly, using the same method of linearly fitting and thermal drift relationship identifying, the results of the separated calibration are obtained as shown in Fig. 5 (panel (a) to panel (e)).

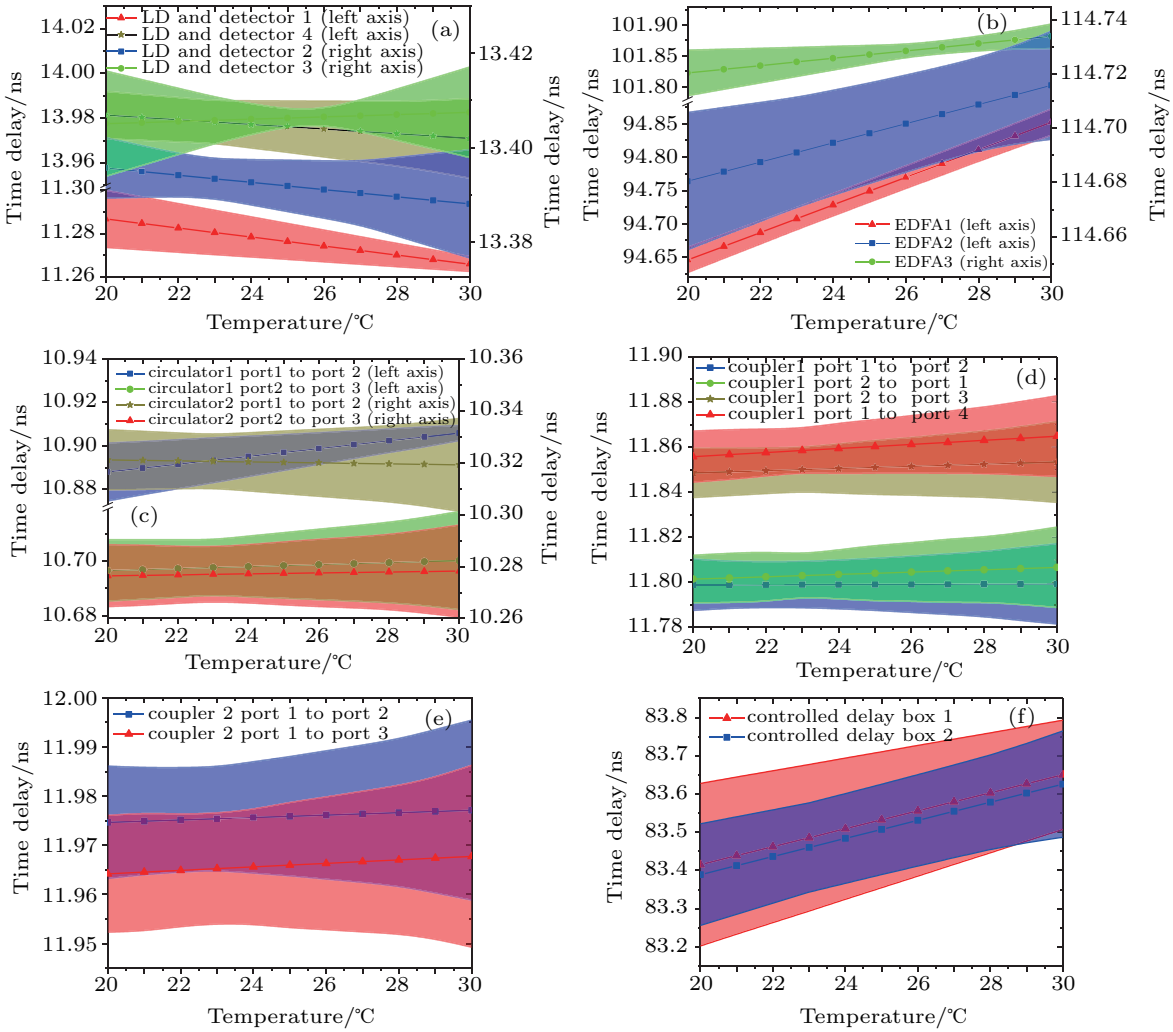


Fig. 5. (color online) Calibration results of all apparatuses: (a) LD and detector pair; (b) EDFAs; (c) optical circulators; (d) optical coupler 2; (e) optical coupler 1; (f) controlled delay boxes.

The time delay of the cables used in Fig. 3 were also measured and are recorded in Table 1. Using these data, the measurement difference between the integrated calibration method and the separated calibration method is shown in Fig. 6. The results of the comparison are promising. The calibration difference of 50 ps in the 20 °C–30 °C temperature range reflects the calibration accuracy of these two methods.

Table 1. The time delay of the cables used in the calibration.

Cable number	1	2	3	4	5	6	7	8+9	8+10
Transfer delay/ns	3.282	3.285	3.364	2.527	2.527	4.805	4.839	3.709	3.702
Uncertainty/ns					0.001				

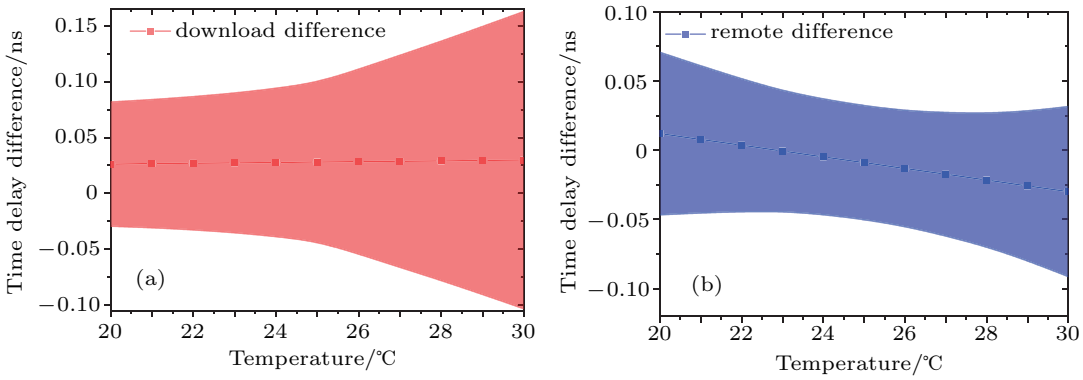


Fig. 6. (color online) The difference between the two calibration methods (integrated and separated): (a) download module calibration difference; (b) remote module calibration difference.

The dead time $T_{\rm dr}(t)$ of the two control delay boxes were also calibrated in the same way. The result is shown in Fig. 5(f). Using the modified control equation $T_{\rm LtoD} = 0.5(T_1+T_2)+T_{\rm asydownload}(t)+T_{\rm dr1}+\Delta T_1$ and $T_{\rm LtoR} = 0.5T_1 + T_{\rm asyremote}(t)+T_{\rm dr2}+\Delta T_2$, the absolute time difference between the local and client modules can be measured and controlled, and timing synchronization among the three modules can be realized. In our lab, the temperature is around 22 °C. Referring to Fig. 4 and Fig. 5(f), we obtain:

$$T_{\rm asydownload}\,(22\ ^\circ{\rm C}) = 6.781 \pm 0.053\ {\rm ns}, \quad (3)$$

$$T_{\rm asyremote}\,(22\ ^\circ{\rm C}) = 58.866 \pm 0.048\ {\rm ns}, \quad (4)$$

$$T_{\rm dr1}\,(22\ ^\circ{\rm C}) = 83.462 \pm 0.199\ {\rm ns}, \quad (5)$$

$$T_{\rm dr2}\,(22\ ^\circ{\rm C}) = 83.436 \pm 0.122\ {\rm ns}. \quad (6)$$

To test the performance of the synchronization system, the absolute time difference between the recovered timing signal and the local clock signal was measured. At first, measurements of T_1 and T_2 were obtained in a single shot using TIC1 and TIC2. The measured results of $0.5(T_1+T_2)$ and $0.5T_1$ were 173150.43 ns and 148530.57 ns, respectively. We can pre-set the demanding time delay of the download and remote modules to $T_{\rm LtoD} = 174000$ ns and $T_{\rm LtoR} = 149000$ ns. ΔT_1 and ΔT_2 can then be set to:

$$\Delta T_1 = 17400 - \frac{1}{2}(T_1+T_2) - 6.781 - 83.642\ {\rm ns}, \quad (7)$$

$$\Delta T_2 = 14900 - \frac{1}{2}T_1 - 58.866 - 83.436\ {\rm ns}. \quad (8)$$

When the round trip fiber transfer delay fluctuation is 60 ns, using the two modified control equations of ΔT_1 and ΔT_2, the measured time difference between the recovered timing signal at the download module and the clock signal at the local module was 173999.894±0.125 ns in one day. The measured time difference between the recovered timing signal at the remote module and the clock signal at the local module was 149000.046±0.100 ns over one day. The difference between the pre-set value and the measured value at the download module and the remote module was 106 ps and 46 ps, respectively. In this way, 100-ps synchronization accuracy was realized.

4. Conclusion and perspectives

We introduced a high precision optical fiber multiple access timing signal synchronization method. The system is able to realize 100-ps magnitude synchronization accuracy and stability for an average of 1 s. High precision timing signals can be acquired at any arbitrary point along the fiber link. The local module only need to measure the round trip delay and broadcast it via ethernet and the compensation is carried out at the download and remote modules, which is different to other multiple access timing signal synchronization methods. Because of the merits such as high precision, low cost, robustness and capacity for future extension, this scheme could be considered as an option for complex time synchronization networks.

References

[1] Turner W "SKA phase 1 system (level 1) requirement specification". Available at: https://www.skatelescope.org/keydocuments/
[2] https://www.ptb.de/emrp/neatft_publications.html
[3] Lau K Y, Lutes G F and Tjoelker R L 2014 *J. Lightw. Technol.* **20** 3440
[4] Predehl K, Grosche G, Raupach S M F, Droste S, Terra O, Alnis J, Legero T, Hänsch T W, Udem T, Holzwarth R and Schnatz H 2012 *Science* **336** 441
[5] Droste S, Ozimek F, Udem T, Predehl K, Hänsch T W, Schnatz H, Grosche G and Holzwarth R 2013 *Phys. Rev. Lett.* **111** 110801
[6] Foreman S M, Holman K W, Hudson D D, Jones D J and Ye J 2007 *Rev. Sci. Instrum.* **78** 021101
[7] Williams P A, Swann W C and Newbury N R 2008 *J. Opt. Soc. Am. B* **25** 1284
[8] Lopez O, Amy-Klein A, Lours M and Chardonnet C 2010 *Appl. Phys. B* **98** 723
[9] Fujieda M, Kumagai M, Nagano S, Yamaguchi A, Hachisu H and Ido T 2011 *Opt. Express* **19** 16498
[10] Wang B, Gao C, Chen W L, Miao J, Zhu X, Bai Y, Zhang J W, Feng Y Y, Li T C and Wang L J 2012 *Sci. Rep.* **2** 556
[11] Jung K, Shin J, Kang J, Hunziker S, Min C K and Kim J 2014 *Opt. Lett.* **39** 1577
[12] Fujieda M, Kumagai M and Nagano S 2010 *IEEE Trans. Ultrason. Ferroelectr. Freq. Control* **57** 168
[13] Gao C, Wang B, Zhu X, Yuan Y B and Wang L J 2015 *Rev. Sci. Instrum.* **86** 093111
[14] Gao C, Wang B, Chen W L, Bai Y, Miao J, Zhu X, Li T C and Wang L J 2012 *Opt. Lett.* **37** 4690
[15] Krehlik P Śiwczynski Ł, Buczek Ł and Lipiński M 2013 *IEEE Trans. Ultrason. Ferroelectr. Freq. Control* **60** 1804
[16] Grosche G 2014 *Opt. Lett.* **39** 2545
[17] Zhang S and Zhao J 2015 *Opt. Lett.* **40** 37
[18] Schediwy S W, Gozzard D, Baldwin K G H, Orr B J, Warrington R B, Aben G and Luiten A N 2013 *Opt. Lett.* **38** 2893
[19] Zhu X, Wang B, Gao C and Wang L J 2016 *Chin. Phys. B* **25** 090601
[20] Wang B, Zhu X, Gao C, Bai Y, Dong J W and Wang L J 2015 *Sci. Rep.* **5** 13851
[21] Chen W, Liu Q, Cheng N, Xu D, Yang F, Gui Y Z and Cai H W 2015 *IEEE Photon. J.* **7** 3
[22] Amemiya M, Imae M, Fujii Y, Suzuyama T and Ohshima S 2005 *IEEE Trans. Fundam. Mater.* **126** 914
[23] Piester D, Rost M, Fujieda M, Feldmann T and Bauch A 2011 *Adv. Radio Sci.* **9** 1
[24] Rost M, Piester D, Yang W, Feldmann T, Wübbena T and Bauch A 2012 *Metrologia* **49** 772
[25] Smotlacha V, Kuna A and Mache W, in *24th European Frequency and Time Forum*, 13–16 April, 2010, Noordwijk, the Netherlands, (IEEE, New York) pp. 1–8
[26] Wu G L, Hu L, Zhang H and Chen J P 2014 *Rev. Sci. Instrum.* **85** 114701
[27] Celano T P, Stein S R, Measander B A and Ramsey B J in *Proceedings of the* 2002 *IEEE International Frequency Control Symposium*, Miami, America, May 29–31, 2002 (IEEE, New York) pp. 510–516
[28] Kim J, Cox J A, Chen J and Kartner F X 2008 *Nat. Photon.* **2** 733
[29] Śiwczynski Ł, Krehlik P and Lipiński M 2010 *Meas. Sci. Technol.* **21** 075302
[30] Krehlik P, Śiwczynski Ł, Buczek Ł and Lipiński M 2012 *IEEE Trans. Instrum. Meas.* **61** 2844
[31] Ning B, Zhang S Y, Hou D, Wu J T Li Z B and Zhao J Y 2014 *Sci. Rep.* **4** 5109
[32] Peng M Y, Callahan P T, Nejadmalayeri A H, Valente S, Xin M, Gruner-Nielsen L, Monberg E M, Yan M, Fini J M and Kartner F X 2013 *Opt. Express* **21** 19982
[33] Jiang Z, Dai Y T, Zhang A X, Yin F F, Li J Q, Xu K, Lv Q, Ren T P and Tang G S 2015 *IEEE Photon. J.* **7** 2
[34] Śiwczynski Ł and Krehlik P 2015 *IEEE Trans. Ultrason. Ferroelectr. Freq. Control* **62** 412
[35] Chen X, Zhang J, Lu J L, Lu X, Tian X S, Liu B, Wu H, Tang T S, Shi K B and Zhang Z G 2015 *Opt. Lett.* **40** 371
[36] Chen X, Lu J L, Cui Y F, Zhang J, Lu X, Tian X S, Ci C, Liu B, Wu H, Tang T S, Shi K B and Zhang Z G 2014 *Sci. Rep.* **5** 18343